Proc. IFAC Workshop on Navigation, Guidance and Control of Underwater Vehicles (NGCUV'2015), Girona, Spain, 28-30 April, 2015

Underwater Single-Beacon Localization: Optimal Trajectory Planning and Minimum-Energy Estimation

Margarida Pedro * **David Moreno-Salinas** ** **N. Crasta** * **António Pascoal** *

* *Laboratory of Robotics and Systems in Engineering and Science (LARSyS), ISR/IST, University of Lisbon, Lisbon, Portugal.*
** *Department of Computer Science and Automatic Control, National Distance Education University, Madrid, Spain.*

Abstract: Single-beacon, range-based AUV localization systems work on the principle that a vehicle may find its position by maneuvering appropriately and acquiring measurements of its successive distances (ranges) to a stationary beacon deployed at a known location. This motivates the study of optimal trajectories to improve the accuracy of the vehicle's position estimate while respecting mission related criteria. In this work, the performance index used to compare different trajectories is the determinant of a properly defined Fisher Information Matrix (FIM). Assuming that heading measurements are available, the problem is studied in 2D, and a class of analytical and numerical solutions are derived. An approach to deal with the case where the initial position of the vehicle is known to lie in a region of uncertainty is also presented. Considering that depth measurements can be obtained, a 3D navigation algorithm consisting of an optimal trajectory planner and a minimum-energy estimator is proposed and its performance assessed via simulation of a practical scientific scenario.

Keywords: Underwater Range-Based Navigation; Single-Beacon Localization; Trajectory Optimization; Fisher Information Matrix

1. INTRODUCTION

A central problem in the field of marine robotics is that of estimating the position of a vehicle in a given inertial reference frame. As applications of marine vehicles become increasingly more diverse, underwater navigation systems are not only required to be reliable and accurate but also affordable and easy to install and operate. For these reasons, single-beacon navigation is steadily emerging as a reduced-cost alternative to conventional acoustic navigation methods such as those at the core of LBL (Long Baseline) and SBL (Short Baseline) systems. However, single-beacon navigation using range measurements introduces some difficulties as well, due to the fact that a single range measurement is clearly not enough to define the vehicle position with respect to a beacon installed at a fixed, known position. Thus, the vehicle must move around and acquire range measurements at different positions, while estimating the displacements in between measurements, in order to compute its own position - which implies that the navigation system is dependent on the type of motion imparted to the vehicle. Motivated by these considerations, this paper is focused on the optimization of trajectories to increase the expected accuracy of single-beacon navigation.

The literature on single-beacon navigation is extensive and defies a simple summary. For early work in the area and a detailed example of the implementation of single-beacon navigation algorithms the reader is referred to Larsen (2000). In what concerns the study of optimal trajectories for single-beacon navigation, the majority of the work reported addresses the study of the observability of the system undergoing specific trajectories, in a deterministic framework; see for instance Gadre and Stilwell (2005) and Crasta et al. (2013). However, these studies do not take into account neither the noise affecting the range measurements nor the uncertainty associated with the estimate of the initial position of the vehicle.

The work presented in this paper follows a different approach, similar to that exposed in Martínez and Bullo (2006), and Moreno-Salinas et al. (2011). We use the determinant of a properly defined FIM as a measure of the best accuracy with which the position of the vehicle can be computed along generic trajectories (using any non-biased estimator), assuming that the measurements are affected by additive Gaussian noise. Besides the quality of the position estimates, other mission related criteria are taken explicitly into account in the trajectory optimization procedure. Namely, energy consumption and how far the actual trajectory of the vehicle deviates from a nominal, desired trajectory. Additionally, we propose a method to deal explicitly with the uncertainty associated with the initial position of the vehicle. The procedures used to compute the trajectories are embodied into an optimal trajectory planner that, in combination with a minimum energy estimator, yields an algorithm for simultaneous trajectory generation and single-beacon navigation. The efficacy of the algorithm developed is assessed with results of simulations of a realistic scientific scenario involving homing in of an underwater vehicle on a deep sea laboratory.

The paper is organized as follows. In Section 2 optimal 2D trajectories are derived, taking into consideration the criteria described above. In Section 3 a 3D single-beacon navigation algorithm is described.

2. 2D SINGLE-BEACON NAVIGATION

2.1 System model

Consider a vehicle moving in 2D while measuring its distance $d(t)$ with respect to a stationary beacon. The motion of the vehicle is controlled through its forward speed $v(t) > 0$ and yaw rate $r(t)$. The location of the beacon is known with respect to some inertial reference frame $\{\mathcal{I}\}$, with North-East-Down orientation (NED). The vehicle has access to the heading angle $\psi(t)$, which provides the orientation of the body-frame with respect to the inertial frame $\{\mathcal{I}\}$. Let the vehicle and the beacon positions in $\{\mathcal{I}\}$ be denoted by $\mathbf{p}(t) = [\, p^n(t) \;\; p^e(t) \,]^{\mathrm{T}}$ and $\mathbf{b_0} = [\, b_0^n \;\; b_0^e \,]^{\mathrm{T}}$, respectively. Without loss of generality, we will assume the beacon to be located at the origin of the reference frame $\{\mathcal{I}\}$, that is, $\mathbf{b}_0 = [\, 0 \;\; 0 \,]^{\mathrm{T}}$. Thus, the distance between the vehicle and the beacon is given by $d(t) = \|\mathbf{p}(t)\|$. The kinematic model of the system with state $\mathbf{x}(t) = [\, p^n(t) \;\; p^e(t) \;\; \psi(t) \,]^{\mathrm{T}}$, input $\mathbf{u}(t) = [\, v(t) \;\; r(t) \,]^{\mathrm{T}}$, and output $\mathbf{y}(t) = [\, d(t) \;\; \psi(t) \,]^{\mathrm{T}}$ over the time-interval $[0, t_f]$ is given by

$$\dot{\mathbf{x}}(t) = \begin{bmatrix} v(t)\cos(\psi(t)) \\ v(t)\sin(\psi(t)) \\ r(t) \end{bmatrix}, \tag{1}$$

$$\mathbf{y}(t) = [\, \|\mathbf{p}(t)\| \quad \psi(t) \,]^{\mathrm{T}}. \tag{2}$$

2.2 Determinant of the FIM

Let z_i with $i = 0, ..., m-1$ denote a set of m measurements of $d(t)$ corrupted by additive noise, obtained at different time instants t_i. Moreover, let d_i with $i = 0, ..., m-1$ denote the actual distances at the time instants of the measurements. The measurement model is given by

$$z_i = d_i + w_i \,, \qquad i = 0, ..., m-1,$$
$$w_i \sim \mathcal{N}(0, \sigma^2) \,, \qquad i = 0, ..., m-1.$$

Assume that the model introduced in Section 2.1 and the measurement model above describe the system perfectly. Additionally, assume that the initial position of the vehicle $\mathbf{p}_0$ is unknown, but that from the set of measurements $\mathbf{z} = (z_0, \ldots, z_{m-1})$ we can obtain an unbiased estimate $\hat{\mathbf{p}}_0$. Under these assumptions, the determinant of the FIM associated with the above problem varies inversely with the volume of the uncertainty ellipsoid of the estimation error. See for example Jauffret (2007) where it is shown that the underlying system is locally observable if the FIM is nonsingular, meaning that trajectories that result from the maximization of the FIM determinant (with $|FIM| > 0$) render the system observable. Classical results in estimation theory (see Van Trees (2001)) dictate that the FIM with respect to the unknown initial position of the vehicle $\mathbf{p}_0$ is given by

$$FIM_{\mathbf{p}_0} \triangleq \mathbb{E}\left\{ [\, J_{\mathbf{p}_0}(\ln \mathcal{L}_{\mathbf{p}_0}(\mathbf{z})) \,] \, [\, J_{\mathbf{p}_0}(\ln \mathcal{L}_{\mathbf{p}_0}(\mathbf{z})) \,]^{\mathrm{T}} \right\}$$

where $J_{\mathbf{p}_0}(\ln \mathcal{L}_{\mathbf{p}_0}(\mathbf{z}))$ denotes the Jacobian of the log-likelihood function of the range measurements with respect to $\mathbf{p}_0$ and $\mathbb{E}$ is the expectation operator. As a consequence, and considering the model introduced in Section 2.1, the determinant of the FIM is given by

$$|FIM_{\mathbf{p}_0}| = \frac{1}{\sigma^4}\left[\sum_{i=0}^{m-1} \left(\frac{p_i^n}{d_i}\right)^2 \sum_{i=0}^{m-1} \left(\frac{p_i^e}{d_i}\right)^2 - \left(\sum_{i=0}^{m-1} \frac{p_i^n}{d_i}\frac{p_i^e}{d_i} \right)^2 \right] \tag{3}$$

where $\mathbf{p}_i = [\, p_i^n \;\; p_i^e \,]^{\mathrm{T}}$ denotes the vehicle's position at t_i.

2.3 Problem setup

The setup for the trajectory optimization considers the model of the system introduced in Section 2.1 under the assumptions below.

Assumption 1. The vehicle speed is constant and the yaw rate is piecewise constant, that is,

$$v(t) \equiv \bar{v},$$
$$r(t) \equiv r_k, \;\; t \in [t_k, t_{k+1}), \;\; k = 0, ..., m-1$$

with $|r_k| \leq r_{\mathrm{b}}$, where r_{b} is a bound on the vehicle yaw rate.

Assumption 2. The time instants at which the inputs may change are given by $t_k = k\,T$, for $k = 0, ..., m-1$, with T the cycle interval. In view of the above, the vehicle position at any t can be written as a function of $\mathbf{p}_0$, ψ_0, $\bar{v}$, $\mathbf{r} = (r_0, \ldots, r_{m-1})$ and T, and is given by

$$\mathbf{p}(t) = \mathbf{p}_0 + \bar{v} \sum_{j=0}^{k-1} \frac{1}{r_j} \begin{bmatrix} \sin(\psi((j+1)\,T)) - \sin(\psi(j\,T)) \\ -\cos(\psi((j+1)\,T)) + \cos(\psi(j\,T)) \end{bmatrix} + \frac{\bar{v}}{r_k} \begin{bmatrix} \sin(\psi(t)) - \sin(\psi(k\,T)) \\ -\cos(\psi(t)) + \cos(\psi(k\,T)) \end{bmatrix}, \tag{4a}$$

$$\psi(t) = \psi_0 + T \sum_{j=0}^{k-1} r_j + (t - k\,T)\, r_k, \tag{4b}$$

$$k = \mathrm{floor}(t/T), \tag{4c}$$

where the function $\mathrm{floor}(x)$ returns the largest integer not greater than x. If any r_k is zero the expression for $\mathbf{p}(t)$ has a singularity, which is removable.

Assumption 3. The time instants at which the range measurements are obtained are given by $t_i = i\,\Delta t$, for $i = 0, ..., m-1$, with Δt the sampling interval.

Assumption 4. The cycle interval of the yaw rate function, T, is a multiple of Δt. We introduce a new tuning parameter c, such that $T = c\,\Delta t$. The vehicle positions and the actual ranges, at the time instants t_i, are given by (4) for $t = i\Delta t$ and $T = c\Delta t$. Hence, the FIM determinant is completely defined as a function of the problem parameters and variables, which are summarized in Table 1. Note that

Table 1. Setup parameters and optimization variables.

setup parameters	$\mathbf{p}_0$, ψ_0, Δt, m, σ, c, $\bar{v}$, r_{b}
problem variables	$r_0, \ldots, r_{N-1}$ with $N = c^{-1}(m-1)$

the speed $\bar{v}$ is a parameter because small AUVs usually keep the speed approximately constant during missions; a typical value is 1.5 $[m/s]$. The bound on the yaw rate is set to $\pi/9$ $[rad/s]$, a typical value for the MEDUSA [1] class of AUVs.

2.4 Maximizing the FIM determinant

The problem of maximizing the FIM determinant including the vehicle dynamics explicitly is too complex for an analytical solution to be obtained for a general scenario. Therefore, we start by looking for a solution in two steps: (i) compute, analytically, the optimal locations for the measurement points neglecting the vehicle dynamics and (ii) find trajectories that cover all the optimal measurement points and check if these are compatible with the vehicle dynamics. As an alternative non-analytic approach,

[1] MEDUSA is an AUV for scientific research developed and operated by the Institute for Systems and Robotics of IST.

we then use numerical methods to compute trajectories that maximize the FIM determinant by including explicitly the vehicle dynamics.

To find the optimal measurement points we maximize the FIM determinant, given by (3), with respect to the measurement points $\mathbf{p}_i$, $0 \leq i \leq m-1$. The problem is solved step-by-step in Moreno-Salinas (2013). The optimality conditions yield

$$\sum_{i=0}^{m-1} \left(\frac{p_i^n}{d_i}\right)\left(\frac{p_i^e}{d_i}\right) = 0,$$

$$\sum_{i=0}^{m-1} \left(\frac{p_i^n}{d_i}\right)^2 = \sum_{i=0}^{m-1} \left(\frac{p_i^e}{d_i}\right)^2 = \frac{m}{2}.$$

Thus, the maximum of the FIM determinant is given by

$$|FIM_{\mathbf{p}_0}|^* = \left(\frac{m}{2\sigma^2}\right)^2$$

which sets an upper bound on the determinant of the FIM that can be achieved with m range measurements in 2D.

In order to characterize the trajectories that pass through the optimal measurement points, first note that the terms p_i^n/d_i and p_i^e/d_i represent the cosine and sine, respectively, of the angle between the axis pointing north and the position vector of the vehicle, α_i. Then, invoking the orthogonality conditions for sines and cosines, from Fourier analysis, we notice that one family of solutions for the optimal measurement points is given by

$$\sum_{i=0}^{m-1} \sin^2(\alpha_i) = \sum_{i=0}^{m-1} \sin^2\left(\frac{2\pi p}{m} i\right), \tag{5a}$$

$$\sum_{i=0}^{m-1} \cos^2(\alpha_i) = \sum_{i=0}^{m-1} \cos^2\left(\frac{2\pi p}{m} i\right), \tag{5b}$$

$$\sum_{i=0}^{m-1} \cos(\alpha_i)\sin(\alpha_i) = 0, \tag{5c}$$

where $p \in \mathbb{N}$. Figure 1 represents the general form of one

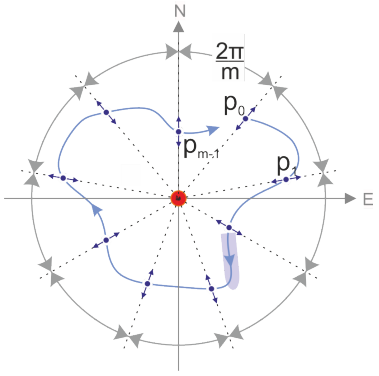

Fig. 1. General form of an optimal solution in 2D.

family of solutions for the problem at hand. From (5a)-(5c) it is clear that the optimality conditions are fulfilled if the optimal measurement points are radially distributed around the beacon; the optimality of the solution does not depend on the distance of the points to the beacon, neither on their time sequence. Additionally, the solution remains optimal (i) if any of these points is replaced by its reflection with respect to the beacon or (ii) if all points suffer an equal rotation centered in the beacon. These two facts show that there are an infinite number of optimal solutions. For a constant turning rate and maintaining a fixed distance to the beacon, an optimal trajectory is obviously a circumference centered at the beacon.

In order to find other solutions/trajectories that respect the constraints on the maneuverability of the vehicle, the dynamics of the latter are now included explicitly in the trajectory optimization. Because of the increased complexity of the optimization problem, numerical algorithms available from the Global Optimization Toolbox of MATLAB are used. Under the assumptions stated at the beginning of this Section, the problem of finding the trajectories that maximize the FIM determinant is equivalent to that of finding the set of m values for the optimization variables that maximize the FIM determinant, that is, compute

$$\max_{r_0,\ldots,r_{m-1}} \quad |FIM_{\mathbf{p}_0}|$$

subject to

$$|r_k| \leq r_{\mathrm{b}}, \qquad \text{for} \quad k = 0, \ldots, N-1 \tag{6}$$

where $|FIM_{\mathbf{p}_0}|$, given by (3), is defined as a function of the optimization variables and setup parameters by (4).

Table 2. Results of the numerical optimization of the FIM determinant.

Scenario	ψ_0 $[rad]$	r_{b} $[rad/s]$	$\sigma^4\lvert FIM\rvert$
1	$\pi/2$	$\pi/9$	64.00
2	0	$\pi/9$	38.00
3	0	$2\pi/9$	59.30

Table 2 shows the results obtained with the numerical procedure for different scenarios, with $\mathbf{p}_0 = (10, 0)$ $[m]$, $\Delta t = 1\,[s]$, $m = 16$, $c = 1$, $\bar{v} = 1.5\,[m/s]$ and the remaining setup parameters defined in Table 2. The maximum dimensionless FIM determinant considering 16 range measurements is $\sigma^4|FIM|^* = 64$. Analyzing Table 2 we see that, for scenario 1, the limits imposed by the vehicle dynamics did not preclude the optimization procedure from finding a trajectory with maximum performance. On the other hand, for scenarios 2 and 3, the constraints imposed on the vehicle maneuverability degrade the navigation system performance (in comparison to the optimal situation). Thus, we conclude that the effect of the limitations of the vehicle maneuverability on the achievable performance depends on the setup parameters, that is, the initial conditions, $\mathbf{p}_0$ and ψ_0, and the parameters m, c, and Δt.

2.5 Minimizing energy consumption

We will now derive trajectories that attempt to simultaneously maximize the FIM determinant and minimize the energy consumption along the trajectory. Stated rigorously, we exploit the so-called Pareto optimal boundary that is often used to examine trade-offs among multiple competing objectives (see Stadler (1988)). The energy criterion is based on very general principles that are in accordance with the kinematic model. Consider that the energy consumption while the vehicle moves is mainly used to overcome the longitudinal drag force F_D and the drag torque τ_D. Because v and r are constant or piecewise constant for the trajectories considered, it follows from simple hydrodynamic principles that $P_F \propto |v|^3$ and $P_\tau \propto |r|^3$ (P_F and P_τ denote the power of drag force and torque, respectively). Neglecting the additional energy spent in changing the yaw rate, the basic model for power consumption is given by $P(t) = \beta\,|\bar{v}|^3 + \gamma\,|r(t)|^3$ with $\beta, \gamma > 0$. Because in the current study the linear speed

is not an optimization variable, the energy criterion for the optimization procedure is given by

$$E = \int_0^{t_f} |r(t)|^3 \mathrm{d}t$$

which, under the assumptions considered for this setup, can be written as

$$E = c\,\Delta t \sum_{j=0}^{N-1} |r_j|^3 - (Nc - m)\ \Delta t\, |r_{N-1}|^3.$$

Combining the energy criterion with the FIM determinant criterion in a single optimization yields a multicriteria optimization problem. In mathematical terms the problem is formulated as

$$\max_{r_0,\ldots,r_{N-1}} \ (\,|FIM_{\mathbf{p}_0}|\,,\ -E\,)$$

subject to (6). To solve this optimization problem we resorted to the Multicriteria Optimization Toolbox from MATLAB.

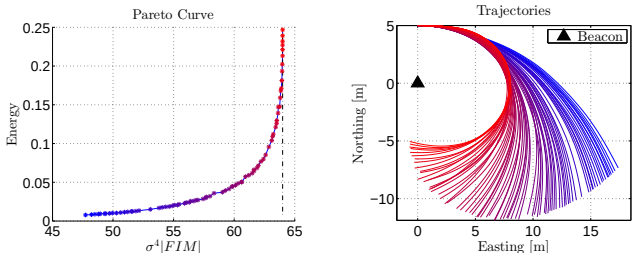

Fig. 2. Numerical results obtained by maximizing the FIM determinant and reducing the energy consumption, simultaneously.

Figure 2 shows the results of the optimization for $\mathbf{p}_0 = (5, 0)\ [m]$, $\psi_0 = \pi/2\ [rad]$, $\Delta t = 1\ [s]$, $m = 16$, $c = 1$, $\bar{v} = 1.5\ [m/s]$ and $r_\mathrm{b} = \pi/9\ [rad/s]$. The plot on the left shows the Pareto optimal solutions and a Pareto curve obtained by connecting the solution points (blue line). The plot on the right shows the trajectories associated to each of the Pareto solutions, using the same color. Note that blue represents trajectories with less energy consumption while red represents trajectories with higher energy consumption by the vehicle. The trade-off between the two objectives of the optimization is very clear: (i) minimizing the energy consumption leads directly to the reduction of the absolute values of the yaw rate, which decreases the vehicle's ability to circumnavigate the beacon, thus reflecting in lower values of the FIM determinant; (ii) notice, however, that the FIM determinant reaches its maximum value while the energy function continues increasing its value, which means that there is a point where increasing the absolute value of the yaw rate does not improve the performance of the navigation system.

2.6 Minimizing the deviation from a nominal trajectory

In a real situation, we expect the underwater vehicle to perform a useful mission while it attempts to estimate its position. Motivated by these requirements, we now address the case where the vehicle is requested to follow a nominal trajectory (defined in accordance with operational requirements), but at the same time is given some freedom to maneuver about this trajectory doing 'persistently exciting' motions to improve the accuracy of the position estimates. We denote the nominal trajectory by $\mathbf{p}_n(t) : [0, t_f] \to \mathbb{R}^2$ and the actual trajectory by $\mathbf{p}(t) : [0, t_f] \to \mathbb{R}^2$, both defined in $\{\mathcal{I}\}$. The deviation from the nominal trajectory $\mathbf{p}_n(t)$ is defined as the integral of the squared position error along the trajectory, that is,

$$\delta = \int_0^{t_f} \|\mathbf{p}_n(t) - \mathbf{p}(t)\|^2\, \mathrm{d}t.$$

The optimization problem can now be formulated as

$$\max_{r_0,\ldots,r_{N-1},\bar{v}} \quad \mu_1\, |FIM_{\mathbf{p}_0}| - \mu_2\, \delta$$

subject to (6) and $0 \le \bar{v} \le \bar{v}_\mathrm{ub}$, with μ_1 and μ_2 as weighting factors. To force the terminal state to approach the desired terminal state we added an appropriate penalty term in the error between the two. Furthermore, we included the forward speed as an optimization variable.

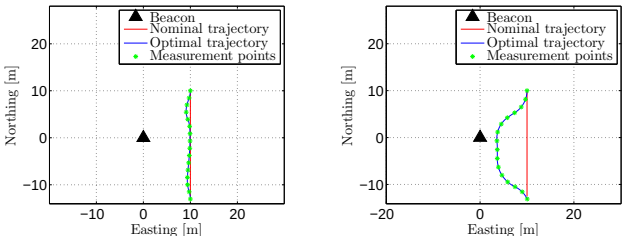

Fig. 3. Numerical results obtained by maximizing the FIM determinant and reducing the deviation from a nominal trajectory for $\mu_1 = 10, \mu_2 = 1$ (left) and $\mu_1 = 20, \mu_2 = 1$ (right).

Figure 3 shows two trajectories resulting from the numerical optimization, for different weighting factors μ_1 and μ_2. The setup parameters are $\mathbf{p}_0 = (10, 10)\ [m]$, $\psi_0 = \pi\ [rad]$, $\Delta t = 1\ [s]$, $m = 16$, $c = 1$, $r_\mathrm{b} = \pi/9\ [rad/s]$, and $\bar{v}_\mathrm{ub} = 2\ [m/s]$; the nominal trajectory is defined by a constant speed $\bar{v}_\mathrm{nom} = 1.5 [m/s]$, $\mathbf{r}_\mathrm{nom} = \mathbf{0}$, and $\psi_\mathrm{nom} = \psi_0$. Obtaining the range measurements along the nominal trajectory, with a sampling interval Δt, yields $\sigma^4|FIM|_\mathrm{nom} = 50.05$, which is already close to the maximum achievable value $\sigma^4|FIM|^* = 64$ (for $m = 16$). Nevertheless, the slight oscillation that we see in the left plot is enough to improve the performance to $\sigma^4|FIM|\big|_{(\mu_1,\mu_2)=(10,1)} = 52.44$. Furthermore, the trajectory in the right plot allows for the performance to reach $\sigma^4|FIM|\big|_{(\mu_1,\mu_2)=(20,1)} = 63.09$, although it deviates considerably from the nominal trajectory. In practice, the trade-off between the two objective functions depends on the requirements of specific missions.

3. SINGLE-BEACON NAVIGATION UNDER UNCERTAINTY IN THE INITIAL POSITION

In this Section we introduce a single-beacon 3D navigation algorithm with range, depth, and heading measurements, consisting of an optimal trajectory planner and a minimum-energy estimator. In the design of the trajectory planner we apply the methods derived in the previous Section, with the required modifications to account for 3D navigation. The model of the system in 3D includes a flight-path-angle input (to control the vehicle vertical position) and the vehicle depth as an output. Additionally, an approach to deal with the problem of having some uncertainty associated with the vehicle initial position is presented. The navigation algorithm is tested in simulation for a practical scenario.

3.1 Uncertainty in the initial position of the vehicle

Assuming that the vehicle horizontal position lies inside an uncertainty region [2], we approached the problem of obtaining an optimal trajectory for navigation by maximizing the worst performance in terms of the FIM determinant inside the region of uncertainty. An alternative would have been to maximize the expected value of the FIM determinant along the uncertainty region. The uncertainty region $\mathcal{U}$ is modeled as a circle with center $c_0 = [\ c_0^n\ \ c_0^e\ ]^{\mathrm{T}}$ and radius r_0. The problem can be formulated as

$$\max_{\mathbf{r}} \min_{\mathbf{p}_0 \in \mathcal{U}} \quad |FIM(\mathbf{p}_0, \mathbf{r})|$$

subject to (6), with the $|FIM|$ defined as a function of $\mathbf{r}$ and $\mathbf{p}_0$ by (3) and (4). Due to the complexity of this problem, we (i) resorted to numerical methods to obtain a solution, and (ii) discretized the uncertainty region $\mathcal{U}$ into a set of points inside and on the boundary of the circle. The performance of the trajectories provided by this procedure depends on the location and dimension of the uncertainty region, and on the setup parameters. Nevertheless, when compared with randomly generated trajectories, the first consistently outscored the latter significantly.

3.2 An algorithm for single-beacon navigation

The navigation algorithm that we propose includes a trajectory planner and a position estimator working in a loop. Its structure is as follows: given a certain initial estimate of the state of the system and the corresponding initial covariance matrix, (i) the trajectory planner provides the vehicle's speed, yaw rate, and flight-path angle commands for an optimal trajectory; (ii) the position estimator observes the outputs of the system (range, depth, and heading) and provides an estimate of the vehicle position and the associated uncertainty and (iii) based on this information the trajectory planner recomputes the optimal trajectory, restarting the loop. For simplicity of exposition, it is assumed that the commands for speed, yaw rate, and flight-path angle are tracked accurately by the vehicle.

Minimum-energy state estimator In what follows we resort to the use of a minimum-energy estimator to compute the position of the vehicle. The reader is referred to Aguiar and Hespanha (2006) for the details, which we omit here. The dynamics of the minimum-energy estimator with estimate vector $\hat{\mathbf{x}} = [\ \hat{p}^n\ \ \hat{p}^e\ \ \hat{p}^d\ \ \hat{d}^2\ ]^{\mathrm{T}}$, are given by

- for $t_i \le t < t_{i+1}$, $i = 0, ..., l$

$$\dot{Q}(t) = -Q(t)\,A(t) - A^{\mathrm{T}}(t)\,Q(t) - Q(t)\,\Gamma\,Q(t) + C_c^{\mathrm{T}}(t)\,R_c^{-1}\,C_c(t)$$

$$\dot{\hat{\mathbf{x}}}(t) = \mathbf{f}(\hat{\mathbf{x}}(t), \mathbf{u}(t)) + Q^{-1}(t)\,C_c^{\mathrm{T}}(t)\,R_c^{-1}\Big(\mathbf{y}_c(t) - \mathbf{h}_c(\hat{\mathbf{x}}(t), \mathbf{u}(t))\Big)$$

- at $t = t_{i+1}$, $i = 0, ..., l-1$

$$Q(t_{i+1}) = Q(t_{i+1}^-) + C_d^{\mathrm{T}}(t_{i+1}^-)\,R_d^{-1}\,C_d(t_{i+1}^-)$$

$$\hat{\mathbf{x}}(t_{i+1}) = \hat{\mathbf{x}}(t_{i+1}^-) + Q^{-1}(t_{i+1})\,C_d^{\mathrm{T}}\,(t_{i+1}^-)\,R_d^{-1}\Big(\mathbf{y}_d(t_{i+1}) - h_d(\hat{\mathbf{x}}(t_{i+1}^-), \mathbf{u}(t_{i+1}^-))\Big)$$

with

$$\mathbf{f}(\hat{\mathbf{x}}(t), \mathbf{u}(t)) = \begin{bmatrix} v(t)\cos(\gamma(t))\cos(\psi(t)) \\ v(t)\cos(\gamma(t))\sin(\psi(t)) \\ v(t)\sin(\gamma(t)) \\ r(t) \end{bmatrix}$$

$$\mathbf{h}_c(\hat{\mathbf{x}}(t), \mathbf{u}(t)) = \begin{bmatrix} p^d(t) \\ \psi(t) \end{bmatrix}$$

$$h_d(\hat{\mathbf{x}}(t), \mathbf{u}(t)) = (p^n(t))^2 + (p^e(t))^2 + (p^d(t))^2$$

$$A(t) = \begin{bmatrix} 0\ 0\ 0 & -v(t)\cos(\gamma(t))\sin(\psi(t)) \\ 0\ 0\ 0 & v(t)\cos(\gamma(t))\cos(\psi(t)) \\ 0\ 0\ 0 & 0 \\ 0\ 0\ 0 & 0 \end{bmatrix}$$

$$C_c(t) = \begin{bmatrix} 0\ 0\ 1\ 0 \\ 0\ 0\ 0\ 1 \end{bmatrix}$$

$$C_d(t) = \begin{bmatrix} 2p^n(t)\ \ 2p^e(t)\ \ 2p^d(t)\ \ 0 \end{bmatrix}$$

and $Q(0) := Q_0 \succ 0$ and $\hat{\mathbf{x}}(0) := \hat{\mathbf{x}}_0$ the initial information matrix and state estimate, respectively; Γ, R_c and R_d are parameters of the filter.

Trajectory planner The trajectory planner is divided in two phases:

i) For a predefined time interval the vehicle moves with the single purpose of improving the position estimate. To this effect we employ the maximization procedure introduced in Section 3.1.
ii) Given a nominal trajectory that the vehicle should follow, the trajectory planner provides a trajectory that stays close to the nominal trajectory, but ensures enough 'excitation' for the estimation procedure. To meet this objective, we employ the optimization procedure introduced in Section 2.6, with proper modifications to consider the system in 3D, with depth measurements available.

Using the position estimate and its covariance provided by the observer, the uncertainty region is defined as a circle in the horizontal plane with center $\hat{\mathbf{p}}$ and radius computed from the Q matrix. When the radius of the uncertainty region duplicates or reduces to half, a new trajectory is re-planned.

3.3 A practical scenario: simulation results

One of the goals in underwater scientific research is to operate, in the near future, several underwater labs to monitor biodiversity, collect data in general, and carry out experiments in situ. An example of these labs is the already existing NOOA Aquarius Reef Base, Shepard et al. (1996), in Florida U.S.A. For deep-waters, one practical difficulty is the access to these labs to service them or to retrieve data from data-storing devices in an affordable manner. For data transferring purposes there is clear advantage in the use of simple AUVs capable of homing in on a beacon installed in the laboratory, docking onto a docking station, and retrieving the required data. This is the scenario where we propose to test the navigation algorithm, in simulation. It consists of an underwater lab located, 1000 meters below the sea surface equipped with an acoustic beacon. An AUV is launched at the see surface with an initial estimate of the state $\hat{\mathbf{x}}_0$ and covariance Q_0^{-1} (with respect to the NED frame with origin at the lab). The AUV homes in on the lab and docks there to collect the available data. To this effect, it uses the navigation algorithm developed in the paper, by measuring its range to the lab. To complete the phase 1 of the algorithm, the vehicle is given 5 minutes to improve the position estimate. For phase 2, the nominal (desired) trajectory consists of three straight lines: (i) one vertical part, that covers half of the vertical distance to the lab; (ii) one part with constant flight-path angle and

[2] The vertical position is known through the depth measurements.

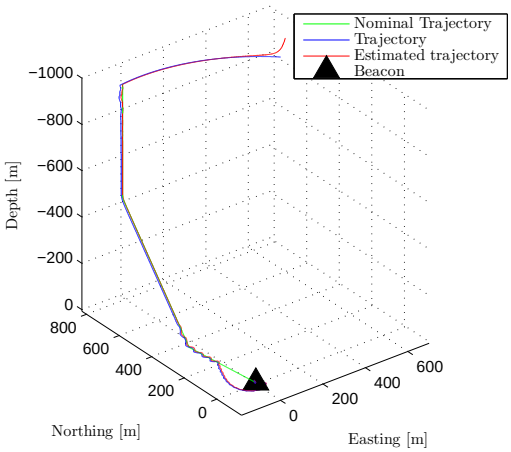

Fig. 4. Simulation results - trajectories.

heading angle; and (iii) one horizontal part with the same constant heading as the previous part, that covers the remaining horizontal distance to the lab. Figure 4 shows the trajectories obtained in simulation with Gaussian noise of variance 10 $[m^2]$ corrupting the range measurements. The filter parameters are $\Gamma = 0$, $R_c = \text{diag}([0.01\ 1])$ and $R_d = 0.01$. The estimates for north and east coordinates are initialized 100 $[m]$ apart from the true coordinates. When the position estimate indicates that the vehicle reached the lab, the true position is 20 $[cm]$ apart. If more precision is required for docking, short-range auxiliary systems can be used, such as cameras.

4. CONCLUSIONS AND FUTURE WORK

The main focus of the paper was on the computation of optimal underwater vehicle trajectories to maximize the information available for single beacon localization. In contrast with previous techniques published in the literature, we addressed explicitly the case where there are competing criteria that involve maximizing the information for localization purposes while at the same time reducing the energy spent in vehicle maneuvering as well as its deviation from a desired, nominal trajectory. Algorithms were developed that allow for the study of the Pareto optimal fronts for the resulting multicriteria optimization problem. Considering that depth measurements can be obtained, a 3D navigation algorithm consisting of an optimal trajectory planner and a minimum-energy estimator was proposed and its efficacy evaluated with the results of simulations of a practical scenario. The results obtained hold promise for practical implementation. Future immediate work will aim at implementing these algorithms and trying them out at sea using an AUV equipped with a ranging device.

5. ACKNOWLEDGMENTS

This work was supported by the EC CADDY project (FP7/ICT/2013/10) and the FCT [PEst-OE/EEI/LA0009/2011]. The second author wishes to thank the 'Ministerio de Economia y Competitividad' for support under project DPI2013-46665-C2-2-R.

REFERENCES

Aguiar, A.P. and Hespanha, J.P. (2006). Minimum-energy state estimation for systems with perspective outputs. *IEEE Transactions on Automatic Control*, 51(2), 226–241.

Crasta, N., Bayat, M., Aguiar, A.P., and Pascoal, A.M. (2013). Observability analysis of 2D single beacon navigation in the presence of constant currents for two classes of maneuvers. In *Control Applications in Marine Systems*, volume 9, 227–232.

Gadre, A. and Stilwell, D. (2005). A complete solution to underwater navigation in the presence of unknown currents based on range measurements from a single location. In *IEEE/RSJ International Conference on Intelligent Robots and Systems, (IROS)*, 1420–1425.

Jauffret, C. (2007). Observability and Fisher information matrix in nonlinear regression. *IEEE Transactions on Aerospace and Electronic Systems*, 43(2), 756–759.

Larsen, M. (2000). Synthetic long baseline navigation of underwater vehicles. In *OCEANS 2000 MTS/IEEE Conference and Exhibition*, volume 3, 2043–2050.

Martínez, S. and Bullo, F. (2006). Optimal sensor placement and motion coordination for target tracking. *Automatica*, 42(4), 661–668.

Moreno-Salinas, D. (2013). *Adaptive Sensor Networks for Mobile Target Localization and Tracking*. Ph.D. thesis, Universidad Nacional de Educacin a Distancia, Spain.

Moreno-Salinas, D., Pascoal, A., and Aranda, J. (2011). Optimal sensor placement for underwater positioning with uncertainty in the target location. In *IEEE International Conference on Robotics and Automation (ICRA)*, 2308–2314.

Shepard, A., Dinsmore, D., Miller, S., Cooper, C., and Wicklund, R. (1996). *Aquarius Undersea Laboratory: The Next Generation*. American Academy of Underwater Sciences (AAUS).

Stadler, W. (1988). *Multicriteria Optimization in Engineering and in the Sciences*, volume 37. Springer.

Van Trees, H.L. (2001). *Detection, Estimation, and Modulation Theory (Part I)*. John Wiley and Sons.